Eksakta : Berkala Ilmiah Bidang MIPA
VOLUME 27 NO 05 2026, pp 859-870
ISSN : Print 1411-3724 — Online 2549-7464
DOI : https://doi.org/10.24036/eksakta/vol27-iss05/745

Eksakta
Berkala Ilmiah Bidang MIPA
http://www.eksakta.ppj.unp.ac.id/index.php/eksakta

Article

Characterization of 304 Stainless Steel Material in Food Tray

Reza Zikri Hadi[1], Andril Arafat[1*], Intan Amita Waluya[1], Zainal Abadi[1], Rifelino[1]

[1]Department of Mechanical Engineering, Faculty of Engineering, Universitas Negeri Padang, Padang, Indonesia

Article Info

Article history :
Received August 16, 2026
Revised September 26, 2026
Accepted September 28, 2026
Published October 30, 2026

Keywords :
Food tray,
stainless steel 304,
characterization,
whole-region AFM

Abstract. Commercial SUS304 food trays produced through forming are expected to maintain appropriate material and surface conditions for food-contact applications. However, physical and visual defects were observed in products from a commercial batch, including a problematic tray. Preliminary SEM-EDS indicated lower-than-specified Ni content, raising an initial suspicion of material-grade deviation; owing to EDS limitations in quantitative alloy analysis, this finding was subsequently verified using OES. This study aimed to identify material-related and post-forming characteristics that may contribute to the observed condition through comparative characterization of problematic and reference food trays. OES confirmed that both samples complied with the specified SUS304 composition, indicating that the low-Ni finding was not confirmed. Median Vickers hardness values were comparable (267 and 271 HV, respectively), although the problematic sample exhibited greater local hardness variability. Whole-region AFM analysis revealed distinct surface roughness classes: N4 (0.15–0.30 μm) for the problematic sample and the finer N2 class (0.04–0.08 μm) for the reference. Overall, the less favorable condition was more strongly characterized by local mechanical and surface heterogeneity than by overall hardness or material grade. These findings highlight the importance of evaluating local mechanical variation and post-forming surface characteristics when investigating defects in commercial deep-drawn stainless-steel products.

This is an open acces article under the CC-BY license.

This is an open access article distributed under the Creative Commons 4.0 Attribution License, which permits unrestricted use, distribution, and reproduction in any medium, provided the original work is properly cited. ©2026 by author.

Corresponding Author :
Andril Arafat
Department of Mechanical Engineering, Faculty of Engineering,
Universitas Negeri Padang, Padang, Indonesia
Email : arafat@ft.unp.ac.id

1. Introduction

The Stamping is a process of forming sheet material or a blank into a cylindrical or box shaped object. The forming process is referred to as deep drawing when the depth exceeds 1.5 times the object's diameter [1-2]. Materials such as steel use stainless (SUS) are suitable for this process due to their ability to withstand high stress and their inherent ductility [3]. Food trays are also manufactured using a same process. The formation of the trays subjects the material to high tensile stress.

In several commercial applications, defects such as wrinkling, tearing, corrosion, and dullness have been identified in commercial SUS304 food trays. These visual and structural failures do not comply with the quality specifications established by the Indonesian National Standard for stainless steel food trays (SNI 9369:2025). To investigate of the cause of these defects, a preliminary chemical composition analysis was performed on defective samples using scanning electron microscopy with energy-dispersive X-ray spectroscopy (SEM-EDS) Therefore, an initial chemical composition analysis using SEM-EDS was conducted on one of the defective product samples. Although the primary metallic elements generally aligned with 304 stainless steel, preliminary internal material test results (Test Certificate No. 181) revealed a sub-standard nickel content ranging from 6.8% to 7.1%.

Nickel is the primary alloying element in 304 stainless steel, serving to stabilize the austenite structure and thereby imparting good ductility, formability, toughness, and corrosion resistance to the material [4-5]. Theoretically, a reduction in nickel content below standard specifications has the potential to decrease austenite phase stability and increase the tendency for strain-induced martensitic transformation (SIMT) during plastic deformation [5-8]. The transformation is reported to increase the work-hardening rate, which, under certain conditions, can affect the material's mechanical properties and formability [4]. Therefore, if a 304 stainless steel product is indicated to have a nickel content lower than specified, further material characterization is required to determine whether this condition is genuinely linked to changes in material characteristics that could explain the appearance of defects in the product.

Observable differences in metallurgical characteristics directly impair mechanical performance during material forming. Less supportive material properties such as reduced ductility and elevated hardness diminish plastic deformability [9-10], which heavily dictates deep drawing success [4-5]. Consequently, the observed product defects likely originated from material incompatibility during the manufacturing stage.

To investigate the alleged issue, material characterization is required to thoroughly evaluate the material's characteristics. Optical Emission Spectrometry (OES) based on ASTM E1086, as mandated by SNI 9369:2025, was conducted to verify alloy compliance. Chemical composition and microhardness values were benchmarked against ASTM A240 standards for SUS304 stainless steel, which specifies both elemental thresholds and mechanical property limits. Furthermore, microhardness testing was employed to assess localized strain hardening induced by forming [3-4],. Non-destructive surface characterization was also performed to evaluate roughness from plastic deformation and tool contact [11-12], as elevated roughness correlates with visual dullness and increased corrosion susceptibility due to micro-valley retention of corrosive media [12-14]. Integrating these three parameters provides a comprehensive baseline for evaluating the finished commercial product.

Although numerous studies have investigated the relationships among chemical composition, mechanical properties, and formability of SUS304 sheet materials, investigations specifically addressing the material and surface characteristics of finished commercial food trays after forming remain limited. Previous studies have commonly examined SUS304 sheet materials before and after forming to characterize material behavior and the changes induced by the forming process. Such studies provide important insights into the relationship between the initial material condition and its response to forming. However, this approach does not necessarily address whether the characteristics observed in a finished commercial product exhibiting product issues are abnormal when compared

with those of a comparable finished product. Therefore, the final formed product itself needs to be investigated directly, particularly when the objective is to assess material and surface characteristics associated with an observed product issue.

This study addresses this gap through a comparative post-forming product failure analysis of finished commercial SUS304 food trays. Rather than tracing material changes from the pre-forming sheet to the formed condition, the present approach focuses directly on the final commercial products and compares a food tray with observed product issues with a comparable food tray without such issues. Chemical composition, microhardness, and surface roughness are characterized to determine whether measurable differences exist between the finished products. This product-level comparison provides a direct assessment of the final formed condition and helps distinguish characteristics specific to the problem product from those also present in a comparable finished product. Accordingly, this study aims to comparatively characterize finished SUS304 food trays with and without observed product issues and to identify differences in their chemical composition, microhardness, and surface roughness relevant to the observed product condition

2. Experimental Section

2.1. Materials

A novel comparative approach is applied in this research. While previous studies generally compared pre-formed sheets with the formed products, the comparative characterization in this study focuses directly on finished commercial products following the forming process [2]. The primary object of this study is an affected commercial SUS304 food tray measuring 280 × 220 × 55.6 mm, designated as Food tray A. For baseline comparison, a commercial food tray without observed issues, measuring 280 × 220 × 44.5 mm, was acquired and designated as Food tray B. The systematic workflow for this post-forming product failure analysis is presented in Figure 1 below..

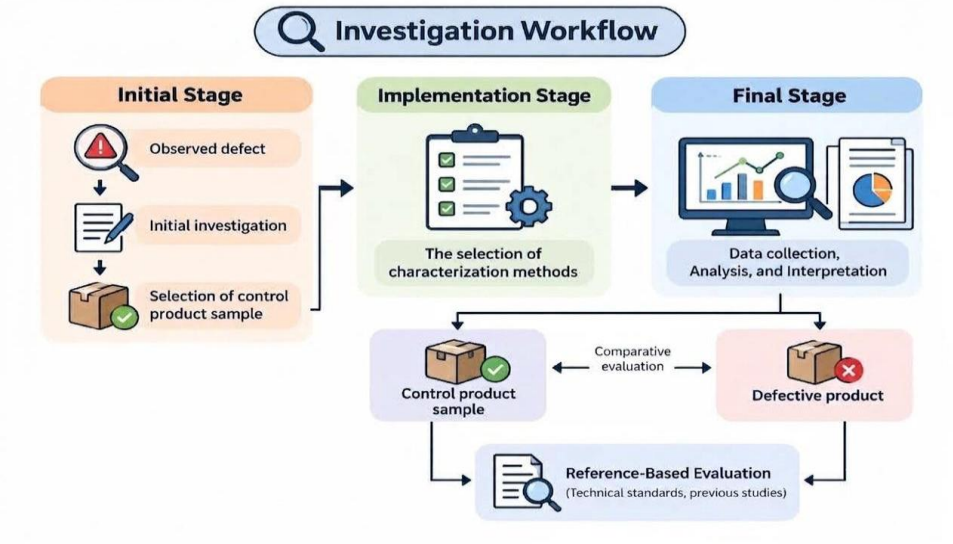


Figure 1. Schematic/Flowchart of research

This research begins with a preliminary investigation of the defective Food tray A using SEM-EDS to assess its apparent material composition and investigate the initial suspicion of grade nonconformity associated with the defects observed in the finished product. The preliminary findings then guided a more comprehensive characterization of Food tray A in comparison with Food tray B as the control product, covering chemical composition, mechanical properties, and surface topography. The results obtained from both food trays were subsequently evaluated against relevant technical standards

(ASTM/JIS/ISO, etc) and previous research to establish a reference-based assessment of their material and surface characteristics. Finally, the findings from the comparative and reference-based evaluations were integrated to identify material- and post-forming-related characteristics that may contribute to the observed failure manifestations. Data analysis was performed using descriptive statistics in conjunction with the results of the material characterization techniques.

2.2. Characterization Methods

The sampling technique in the context of this research in the form of test samples (specimens) in this study is non-probability sampling. The selection of the area for material characterization was done using a mixed technique, namely convenience and purposive sampling. The sampled areas of the Food tray are shown in Figure 2.

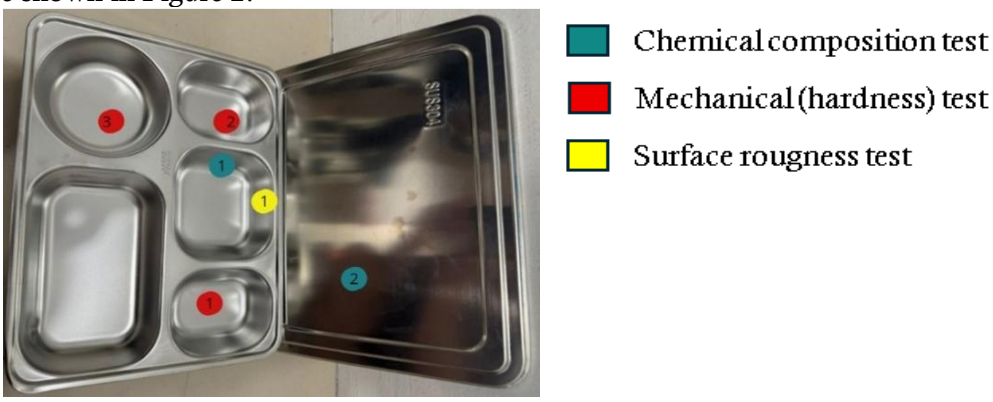


Figure 2. The Product Areas for Material Characterization

The determination of the observation area for the material composition value is based on the principle of convenience, where the availability of the test specimen area must be flat and the testing cost efficiency is lower [15]. The observation area for mechanical performance in the form of material hardness is conducted purposively. As reported in previous studies [2-3], the base of the food tray undergoes the least deformation, making it an ideal region to evaluate the work hardening level of both product samples against the standard stainless steel blank (JIS Standard ≤200HV). The observation area for surface characteristics, such as roughness, is also conducted based on certain considerations (purposive), where the wall area has the maximum deformation level during its formation, as reported in previous studies, thereby significantly increasing the surface roughness values [3],[11-12]. Thus, the product wall area becomes an ideal candidate for surface roughness characterization in response to initial findings of a dull appearance as an indication that the material has a higher roughness level. However, both types of techniques (convenience & purpose) are susceptible to researcher bias and cannot be generalized [15].

Therefore, various characterization methods are combined to provide objective supporting evidence, enabling the reconstruction of product issue mechanisms without relying on population generalization. Instead of pursuing broad statistical generalization, this investigation directly compares the localized defective tray against an unblemished reference sample from a distinct production batch (identified by labeling and slight geometric variations). Integrating this external benchmark with established literature on failure mechanisms yields a direct, mechanistic explanation for the physical degradation, thereby validating the initial problem identification.

2.2.1 Characterization preparation

The test samples were cut using fine shearing with minimal deformation. The dimensions of the test specimens for each type of Food tray are shown in the Figure 3.

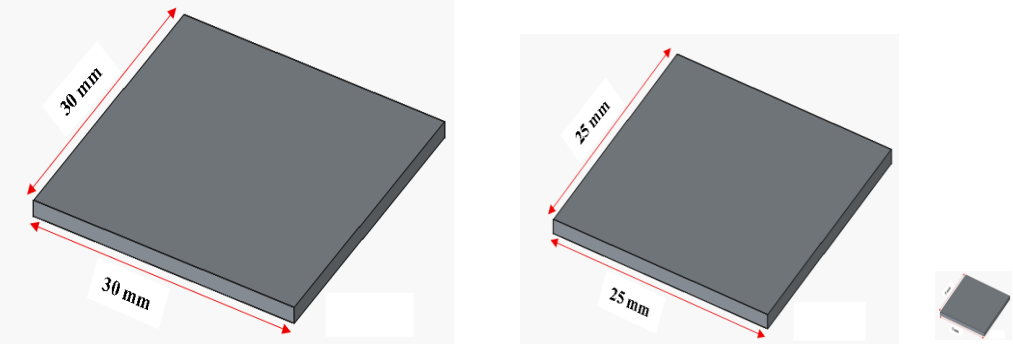


Figure 3. Dimension of specimens. A) Chemical composition test (30x30mm), B.) Surface roughness test (25x25mm), C.) Hardness test (5x5mm).

Based on Figure 3 above, both food trays were cut using aviation snips according to the area of each type of test conducted. The thickness of the test specimen depends on the area of the test sample. The measurement of the food tray's thickness was conducted 10 times using a micrometre with an accuracy of 0.001 mm, randomly distributed across the base, walls, and lid of the food tray. Table 1 below shows the thickness values for each area on both food trays.

Table 1. Specimen thickness based on the Testing Area

Area	Thickness (mm)	
	Food tray A	Food tray B
Bottom	0.28	0.28
Wall	0.32	0.35
Lid	0.34	0.37

Specifically for sample preparation in material hardness testing, the cold mounting technique is performed first. This is followed by polishing until a mirror-like finish is achieved. As for other test samples, the test specimens are soaked in distilled water in an ultrasonic cleaner for 20 minutes. Subsequently, dry them at room temperature.

The chemical composition of the material was tested according to ASTM E1086 using a Bruker QM4 Polo Spark Optical Emission Spectroscopy (OES) equipped with a multivision optical system (wavelength range 130–785 nm). OES testing was limited to two specimens, with each receiving three closely spaced spark points. For mechanical properties, microhardness was characterized per ASTM E384-17 using an FM-800 Microvicker Hardness Tester under a 100 gf load and a 12-second dwell time. Three specimens were tested for each Food tray type (A and B), with three indentations per specimen, yielding nine replicated data points on the product base for each tray type. Meanwhile, surface topography was scanned using Atomic Force Microscopy (AFM) in contact mode at a scan speed of 0.5 Hz over a 40 × 40 μm² area in accordance with ISO 25178. Notably, AFM topographical characterization was limited to a single AFM map.

2.2.2 Data Analysis

To ensure the validity of the measurement results, all material characterization tests were conducted using calibrated instruments and in accordance with relevant international standards, namely ASTM E1086 for chemical composition analysis, ASTM E384-17 for hardness testing, and ISO 25178 for surface roughness measurement. The quantitative data obtained from the material characterization were analyzed descriptively to characterize and interpret the defects identified in the product, which constitute the background and motivation for this study.

The chemical composition was analyzed by comparing the elemental concentrations obtained from OES measurements of Food Trays A and B with the ASTM A240 specifications for Type 304 stainless steel. The material characteristics were interpreted by relating the elemental composition to the measured hardness (HV) of each product. If the initial indication of a nickel content below the specified alloy range in Food Tray A was confirmed, this finding would support the initial premise of the study. Conversely, if both products exhibited comparable concentrations of the principal alloying elements, Cr and Ni, consistent with the nominal 18Cr–8Ni composition specified by ASTM A240, this would indicate that material composition was not the factor responsible for the observed forming failure.

Mechanical performance was evaluated based on hardness data obtained from nine measurement points and visualized using box-and-whisker plots. The hardness data (HV) were interpreted based on the median values and the distribution patterns shown in the boxplots, with Food Tray B (control sample) serving as the reference for evaluating manufacturing consistency and the material response to the forming process. The observed trend in mechanical performance, represented by the median HV values of Food Trays A and B, was also compared with findings from previous studies investigating the deformation behavior of SUS304 products produced through deep drawing.

Subsequently, the AFM topography data were processed using Park Systems XEI software through a whole-region analysis of the surface topography over a measurement area of 40 × 40 μm². The topography data, with a resolution of 256 × 256 pixels, were analyzed over the entire measurement area to characterize the distribution of surface heights, represented by the skewness (Rsk) and kurtosis (Rku) parameters. The Rsk value was used to describe the tendency of the topographic distribution toward the predominance of peaks or valleys, whereas Rku characterized the sharpness or flatness of the surface-height distribution. In addition, the arithmetic mean roughness (Ra) was used to represent the overall surface roughness and was subsequently classified into roughness grades N1 to N12 according to ISO 1302. This whole-region analysis was employed to provide a quantitative representation of the surface topographic characteristics across the entire measurement area, thereby enabling an objective evaluation of the differences in topographic characteristics and roughness grade between the two samples.

3. Results and Discussion

Material composition testing aims to confirm the suitability of the Stainless Steel 304 grade used. The results of the composition testing can be seen in Table 2 below.

Table 2. The Elemental Composition of Sample

Elements	Elemental Weight Total Percentage (wt%)				ASTM A240
	Food tray lid (A)	Food tray lid (B)	Food tray A	Food tray B	
Carbon	0.042	0.042	0.037	0.044	0.07
Silicon	0.233	0.407	0.328	0.357	0.75
Phosphorus	0.017	0.019	0.013	0.016	0.045
Sulphur	0.014	0.023	0.014	0.015	0.030
Chromium	19.07	18.28	18.92	19.33	17.5-19.5
Manganese	0.869	1.266	0.888	1.111	2.00
Iron	71.21	71.22	71.02	70.42	balance
Nickel	8.049	8.227	8.268	8.166	8.0-10.5

According to the chemical composition testing in Table 2, both food trays meet the specifications of SUS304 stainless steel. The primary elemental concentrations show no significant differences between the two samples, confirming that both trays maintain an optimal nickel content of approximately 8%

for the deep drawing process [4]. Consequently, the hypothesis that variations in nickel content influence mechanical performance is not supported. Furthermore, the initial nickel concentration obtained via semi-quantitative EDS analysis was refuted by standard Optical Emission Spectrometry (OES). This discrepancy arises from the inherent physical limitations of EDS in dense Fe-Cr matrices, where excitation volume interaction, matrix absorption effects, and local surface topography distort measurement accuracy [16]. Additionally, spectral peak overlaps among adjacent transition elements (Cr, and Ni) introduce high relative measurement errors in EDS [17-18], whereas bulk volumetric techniques such as OES provide significantly higher quantitative accuracy and precision for major alloying elements [16],[19].

The following section focuses on the material hardness test results. Hardness testing was conducted to evaluate the local mechanical characteristics of the two products, particularly because Food Tray A exhibited indications of defects in the formed product. In this study, a higher hardness value was considered one of the indicators of a material condition that may be more susceptible to forming-related failure, as increased hardness can be associated with greater work hardening and reduced capacity for plastic deformation. The material hardness results are presented in Figure 4..

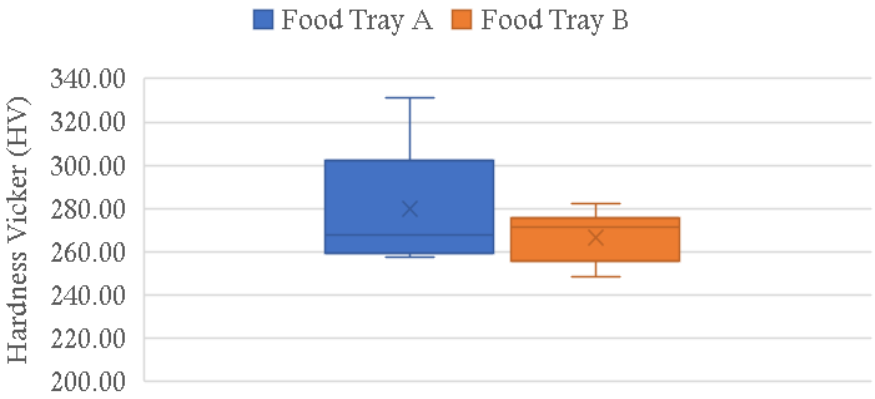


Figure 4. Boxplot of Microvicker hardness values for Food tray A and Food tray B

The local mechanical response can be evaluated based on the distribution of Vickers hardness values presented in the boxplot (Figure 4). Food Tray B, serving as the control sample, exhibited a narrower distribution of HV values, whereas Food Tray A showed a wider distribution. Although the median hardness of Food Tray B was slightly higher than that of Food Tray A (271 HV < 267 HV), Food Tray A exhibited a higher mean hardness (279.80 HV > 266.4 HV). The difference between the median and mean hardness values for Food Tray A indicates a distribution influenced by relatively high hardness measurements, including several values exceeding 300 HV. Therefore, the results do not indicate that Food Tray A had a higher overall hardness level than Food Tray B. Rather, the more prominent characteristic of Food Tray A was its greater local hardness variation, indicating a more heterogeneous mechanical response compared with the control sample.

The locations corresponding to higher hardness measurements may represent regions that experienced more intensive deformation and work hardening [20-23]. Such conditions can reduce the local capacity for plastic deformation and potentially increase susceptibility to cracking if these regions undergo further deformation or sufficiently high loading. Accordingly, the findings shift the interpretation of Food Tray A's susceptibility to failure from its overall hardness level toward the local variation in hardness and the degree of local work hardening developed during the forming process.

In deep-drawn products, the degree of work hardening may vary across different regions of the formed geometry. Regions such as the product walls that undergo greater plastic deformation may exhibit increased dislocation density, grain elongation, and more pronounced strain-induced

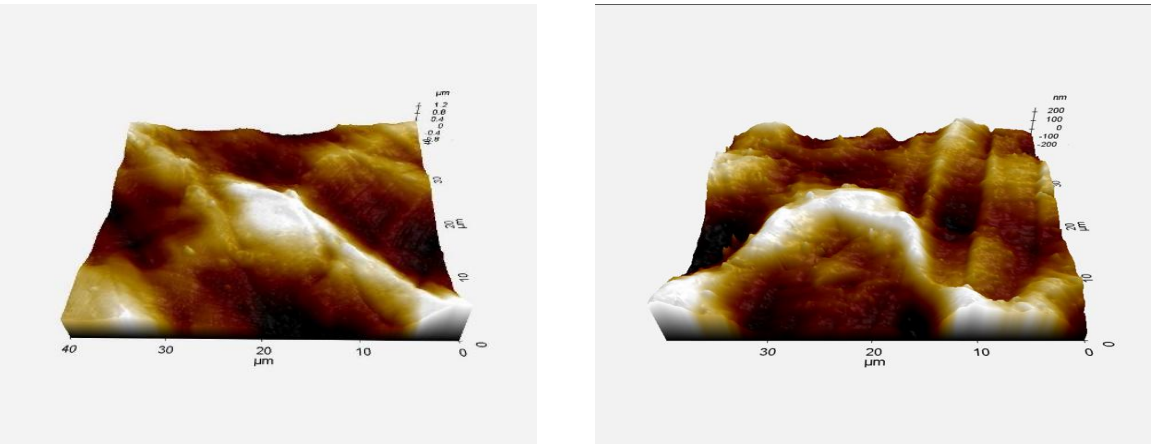
martensitic transformation, resulting in higher hardness [20],[24]. In contrast, regions subjected to relatively lower levels of plastic deformation, such as the product bottom, may exhibit a different degree of strain hardening. Therefore, hardness measurements in this study were focused on the bottom region to ensure that Food Trays A and B were compared at approximately equivalent geometric locations. The hardness trends observed in the bottom regions of deep-drawn SUS304 products, together with reported reference values, are presented in Table 3.

Table 3. Mechanical Performance of SUS304 Products

Product	HV	Reference
Blank SUS304	≤200	JIS Standard
SUS304 deep drawing product 1	258	[3]
SUS304 deep drawing product 2	268	[2]
Food tray A	271	This study
Food tray B	267	This study

As shown in Table 3, the median hardness values of Food Trays A and B (267 and 271 HV, respectively) were comparable to or higher than the hardness values reported in previous studies of SUS304 deep-drawn products, which ranged from 258 to 268 HV. Although the products differed in geometry and configuration, the comparable hardness levels suggest that the six-compartment food tray, with its relatively complex geometry, warrants particular attention in optimizing the forming process.

These mechanical characteristics should be considered together with the visual defects observed on the material surface, which may be associated with increased surface roughness resulting from localized deformation during forming. Figure 3 presents the three-dimensional (3D) surface topography of the two samples.



A B

Figure 3. Surface topography 3D characterization result. A) Food tray A specimen testing, B) Food tray B specimen testing

The surface topographies of Food Trays A and B shown in Figure 3 reflect a combination of the initial surface characteristics of the metal sheets (e.g., 2B or BA surface finishes) and topographical changes occurring during forming, including plastic deformation during the deep-drawing process [25-26]. Because the initial surface finishes of the two products were unknown and were not specifically characterized in this study, their contributions to the final topography cannot be quantitatively separated from those associated with the forming process. Therefore, the discussion focuses on the

observed topographical characteristics and their potential relationship with plastic deformation during deep drawing. To further quantitatively characterize the observed differences in surface topography, the minimum and maximum surface heights, together with the Ra, Rsk, and Rku parameters, were obtained through whole-region analysis of the AFM surface maps and are summarized in Table 4.

Table 4. Roughness parameters

Surface	Region	Min (μm)	Max (μm)	Ra (μm)	Rsk	Rku
Food tray A	Whole (40 × 40 μm²)	-0.89	1.4	0.08	0.504	3.5
Food tray B	Whole (40 × 40 μm²)	-0.23	0.29	0.21	0.294	2.5

Both Food Tray A and Food Tray B exhibit surface profiles dominated by peaks (Rsk > 0) with asymmetric characteristics. However, the degree of surface asymmetry is greater in Food Tray A than in Food Tray B (0.504 > 0.294). Food Tray A exhibits a leptokurtic surface distribution, characterized by highly pronounced peaks and deep valleys (Rku > 3). In contrast, Food Tray B exhibits a platykurtic distribution, characterized by broader, flatter, or more rounded peaks and valleys (Rku < 3).

A deformation mechanism that can increase surface roughness occurs when the material is subjected to stretching, during which relatively large grains may undergo random rotation and displacement [8],[27]. Such grain movements can generate microscale undulations on the surface, which manifest as an orange-peel effect in the context of sheet metal forming [28-30]. Surface roughening not only affects the aesthetic appearance of the product but may also act as a site for strain localization, potentially promoting material failure through localized necking and subsequent fracture.

This anomalous surface condition is strongly suspected to be present in Food Tray A, which exhibits greater asymmetry and highly pronounced peaks accompanied by deep valleys (Rku > 3). High local strain may contribute to irregular grain orientation, resulting in a very deep valley (-0.89 μm) adjacent to a pronounced surface peak (1.4 μm). Conversely, finer grains may improve mechanical performance during sheet metal forming [12],[31-32]. Food tray B exhibits broader, flatter, or more rounded peaks and valleys. This condition may reflect a more uniform surface deformation, thereby limiting the formation of extreme-amplitude valleys and peaks such as those observed in Food tray A. Overall, the average surface roughness (Ra) of the two sample types falls into different surface roughness grades. This difference in surface classification is presented in Table 5.

Table 5. Comparison of Surface Characteristics of Samples

Sample	Ra (μm)	Surface Rougness Level	Value Range (μm)
Food tray A	0.21	N4	0.15-0.30
Food tray B	0.08	N2	0.04-0.08

The difference in surface roughness grade, alongside the mechanical deformation behavior, may provide a strong indication of susceptibility to corrosion initiation [14],[33]. Food Tray A falls within the N4 roughness grade, whereas Food Tray B exhibits a smoother surface classified as N2. Because severe mechanical deformation can induce microstructural defects and higher dislocation densities that accelerate localized attack, deformation history plays a crucial role in initiating corrosion [34]. Although, theoretically, a higher surface roughness (Ra) increases the effective surface area and the number of microscale cavities that act as potential initiation sites, this study did not perform electrochemical, potentiodynamic, or salt spray testing. Therefore, any implications regarding corrosion remain speculative and are based solely on the existing literature, particularly in relation to the corrosion observed in the background of this study.

Optimization of the forming of compartmented food trays is not limited to material characteristics alone; the process parameters employed during forming should also be considered. The identified defects may be associated with process parameters such as lubricant type, punch speed, and blank-holder pressure [35-36]. Previous research has reported that appropriate combinations of lubrication conditions, punch speed, and blank-holder pressure can significantly influence the forming performance of deep-drawn products, with specific parameter combinations providing more favorable forming conditions [4],[36-38]. In the context of the present study, the evaluation focuses on the material characteristics of the formed products, whereas the specific relationship between these characteristics and variations in forming-process parameters may be further investigated to complement the interpretation of the observed product characteristics.

4. Conclusion

Overall, the findings indicate that the less favorable condition of Food Tray A is more strongly characterized by local mechanical and surface heterogeneity than by its overall hardness or material grade. The greater hardness variability may indicate non-uniform local plastic deformation and associated work hardening during forming, while the pronounced orange-peel-like topography may reflect heterogeneous deformation among grains with different crystallographic orientations. Thus, the hardness variability and surface topography can be interpreted as two manifestations of non-uniform plastic deformation at different length scales. These findings highlight the importance of evaluating local mechanical variation and post-forming surface characteristics, rather than relying solely on nominal material grade or overall hardness, when assessing the condition of commercial deep-drawn stainless-steel products.

Further optimization of the deep-drawing process for food tray products may be developed through a finite element analysis (FEA) approach by considering the interactions among process parameters, strain distribution, and material characteristics at deformation locations. This approach may also be extended by considering the microstructural conditions in strain-localized regions and surface roughness characteristics as factors that may potentially influence the mechanisms of failure initiation.

References

[1] Ikumapayi, O. M., Afolalu, S. A., Kayode, J. F., Kazeem, R. A., & Akande, S. (2022). A concise overview of deep drawing in the metal forming operation. *Materials Today: Proceedings, International Conference on Materials, Processing & Characterization (13th ICMPC)*, 62, 3233–3238.

[2] Lu, H., Tian, W., & Xu, J. (2019). Analysis of Surface Cracking Defect of 304 Stainless Steel Deep Drawing Products. *Francis Academic Press*, UK, 2(1), 41–47.

[3] Salhana, B. S., Sajuri, Z., & Kamil, B. S. (2015). Effects of deep drawing process in microstructure of stainless steel S304. 125.

[4] Andrea Casaroli, Edoardo Scabini, Marco V.Boniardi, Riccardo Gerosa, & Barbara Rivolta. (2025). Optimization of austenitic and ferritic steels for deep drawing. *Part 1: Metallurgical and mechanical analyses*. 20, 104–123.

[5] Liu, T., Mukhopadhyay, S., Li, C.-H., Li, T., Ren, Y., Singh, P., & Devaraj, A. (2025). The impact of nickel concentration and stacking fault energy on deformation mechanisms in high-purity austenitic Fe-Cr-Ni alloys. *Materials Characterization*, 224, 115046.

[6] Wong, A. (2022). Modelling the stability and transformation kinetics of retained austenite in steels. *Materials Science and Technology*, 38(11), 676–688.

[7] Sohrabi, M. J., Mehranpour, M. S., Heydarinia, A., Kalhor, A., Lee, J. H., Mirzadeh, H., Mahmudi, R., Parsa, M. H., Rodak, K., & Kim, H. S. (2024). Deformation-induced martensitic transformation kinetics in TRIP-assisted steels and high-entropy alloys. *Acta Materialia*, 280, 120354.

[8] Kijima, R., Jin, M., & Thipprakmas, S. (2026). Multi draw radius (MDR) die application for orange peel prevention in cylindrical deep-drawn cup. *Journal of Manufacturing Processes*, 170, 127–137.
[9] Lüder, S., Lachmann, L., Kunke, A., Leonhardt, A., Barthel, V., & Kräusel, V. (2022). Prediction of Material Failure in Incremental Sheet Metal Forming. *Engineering Proceedings*, 26(1), 19.
[10] Wang, H., Niu, Q., & Yan, Y. (2024). Study of Anisotropic Behavior in Sheet Metal Forming. *Materials*, 17(9),
[11] Szewczyk, M., Szwajka, K., & Trzepieciński, T. (2022). Frictional Characteristics of Deep-Drawing Quality Steel Sheets in the Flat Die Strip Drawing Test. *Materials*, 15(15), 5236.
[12] Nie, N., Su, L., Deng, G., Li, H., Yu, H., & Tieu, A. K. (2021). A review on plastic deformation induced surface/interface roughening of sheet metallic materials. *Journal of Materials Research and Technology*, 15, 6574–6607.
[13] Gorji Kandi, S., Panahi, B., & Zoghi, N. (2022). Impact of surface texture from fine to coarse on perceptual and instrumental gloss. *Progress in Organic Coatings*, 171, 107028.
[14] Rossi, S., Leso, S. M., & Calovi, M. (2024). Study of the Corrosion Behavior of Stainless Steel in Food Industry. *Materials*, 17(7), 1617.
[15] M. Jainuri, S.Pd., M.Pd, Awatif, S,Pd.,MPd, Ade Susanti, S.Pd., M.Pd, Sugeng Riyadi, S.Si.,M.Pd, Hasmawati, S.Pd., M.Pd, & Leni Marlina, M.Si. (2026). *STATISTIKA DESKRIPTIF: Konsep Dasar dan Aplikasi Teknologi* (Egydia Alfariza R.). Hira Institute.
[16] Cipriano, A., Malfatti, C. de F., Casagrande, H. C., Daleffe, A., Castelan, J., & Possamai, P. H. M. (2025). Analysis of the Microstructure and Mechanical Properties of Austenitic Stainless Steel 310 Manufactured via WAAM. *Materials*, 18(16), 3855.
[17] Garzón, C. M., Cruz, J. P. N., Noreña, J. K., Pineda, E. F., & Cachaya, J. S. (2022). Effects of Variations in Operating Conditions on the Preci-sion and Accuracy of Standardless Elemental Analysis of Stainless Steel by SEM-EDS. *Ingeniería e Investigación*, 43(1), e94361.
[18] Giunto, A., Fei, Y., Nevatia, P., Rendy, B., Szymanski, N., & Ceder, G. (2026). Accurate SEM-EDS Quantification, Automation, and Machine Learning Enable High-Throughput Compositional Characterization of Powders. *Research Square.*
[19] Seidel, P., Ebert, D., Schinke, R., Möckel, R., Raatz, S., Chao, M., Niederschlag, E., Kreschel, T., Gloaguen, R., & Renno, A. D. (2021). Comparison of Elemental Analysis Techniques for the Characterization of Commercial Alloys. *Metals*, 11(5), 736.
[20] Maboudi Far, N., Mehdinavaz Aghdam, R., Mirzadeh, H., Gharibi Asl, F., & Najjari, A. (2026). Strain-induced martensitic transformation and mechanical properties of additively manufactured AISI 316L austenitic stainless steel. *Materials Chemistry and Physics*, 354, 132219.
[21] Ennis, B. L., Jimenez-Melero, E., Atzema, E. H., Krugla, M., Azeem, M. A., Rowley, D., Daisenberger, D., Hanlon, D. N., & Lee, P. D. (2017). Metastable austenite driven work-hardening behaviour in a TRIP-assisted dual phase steel. *International Journal of Plasticity*, 88, 126–139.
[22] Andrade, M. S., Gomes, O. A., Vilela, J. M. C., Serrano, A. T. L., & Moraes, J. M. D. de. (2004). Formability evaluation of two austenitic stainless steels. *Journal of the Brazilian Society of Mechanical Sciences and Engineering*, 26, 47–50.
[23] Muñoz, J. A., Komissarov, A., Avalos, M., & Bolmaro, R. E. (2020). Mechanical and microstructural behavior of a heterogeneous austenitic stainless steel processed by Equal Channel Angular Sheet Extrusion (ECASE). Materials Science and Engineering: A, 792, 139779.
[24] Zhu, L., Dong, Z., Cai, G., Li, Y., & Cui, Z. (2026). The effect of cold deformation on crevice corrosion and stress corrosion cracking behavior of 304 stainless steel. *Engineering Failure Analysis*, 186, 110515.

[25] Cai, Y., Wang, X., & Du, Y. (2022). Surface Roughening Behavior of the 6063-T4 Aluminum Alloy during Quasi-in Situ Uniaxial Stretching. *Materials*, 15(18), 6265.
[26] Trzepieciński, T., Najm, S. M., Oleksik, V., Vasilca, D., Paniti, I., & Szpunar, M. (2022). Recent Developments and Future Challenges in Incremental Sheet Forming of Aluminium and Aluminium Alloy Sheets. *Metals*, 12(1), 124.
[27] Adelkhani, A. (2021). Experimental and numerical investigation of effects of sheet thickness and grain size on deep drawing of square parts. *Journal of Mechanical Science and Technology*, 35(11), 5143–5149.
[28] Oleksik, V., Trzepieciński, T., Szpunar, M., Chodoła, Ł., Ficek, D., & Szczęsny, I. (2021). Single-Point Incremental Forming of Titanium and Titanium Alloy Sheets. *Materials*, 14(21), 6372.
[29] Hussain, G., Hassan, M., Wei, H., Buhl, J., Xiao, M., Iqbal, A., Qayyum, H., Riaz, A. A., Muhammad, R., & Ostrikov, K. (Ken). (2023). Advances on Incremental forming of composite materials. *Alexandria Engineering Journal*, 79,308–336.
[30] Arinbjarnar, Ú., Christiansen, R. J., Knoll, M., Pantleon, K., Jellesen, M. S., & Nielsen, C. V. (2023). Strain-Induced Surface Roughening of Thin Sheets and Its Effects on Metal Forming and Component Properties. *Journal of Manufacturing and Materials Processing,* 7(5), 174.
[31] Zhao, M., Wu, H., Lu, J., Sun, G., & Du, L. (2022). Effect of grain size on mechanical property and corrosion behavior of a metastable austenitic stainless steel. *Materials Characterization*, 194, 112360.
[32] Han, J., Zheng, W., Chen, Q., Sun, J., & Xu, S. (2022). Study on Size Effect of Surface Roughness Based on the 3D Voronoi Model and Establishment of Roughness Prediction Model in Micro-Metal Forming. *Coatings*, 12(11), 1659.
[33] Syafei, N. S., Rizki, S. S., Suryaningsih, S., & Hidayat, D. (2019). Comparison of Corrosion Rate in the Environment of 10% Acetic Acid solution with different Deflection. *EKSAKTA: Berkala Ilmiah Bidang MIPA*, 20(2), 84–93.
[34] Behera, A., Behera, B., Sahoo, D. K., Pattnaik, A., Barik, K. N., Mallick, P., Bhuyan, S., Mishra, S. C., & Behera, A. (2021). Effect of Cold Work on Microstructure and Corrosion Properties of 304L Stainless Steel. In P. Pant, S. K. Mishra, & P. C. Mishra (Eds.), *Advances in Mechanical Processing and Design* (pp. 433–439). Springer.
[35] Li, Y., Xu, J., & Luan, B. (2025). Investigation on Strain-Forming Limits and Manufacturing Optimization of a Single Deep-Drawing Process Concerning 304 Stainless Steel's Thin Sheet. *Metals*, 15(9), 1008.
[36] Atal, A. S., & Shete, M. T. (2013). Material Deformation and Wrinkling Failure in Deep Drawing Process by Finite Element Approach: A Review. *International Journal of Engineering Research*, 2(12).
[37] Celik, I., Şensoy, A. T., Seven, G., & Cicek, D. (2025). Improving Deep Drawing Quality of DD13 Sheet Metal: Optimization of Process Parameters Using Box–Behnken Design. *Materials*, 18(7), 1424.
[38] Joun, M. S., Park, M. C., Heo, Y., & Kim, D. H. (2025). A Review of Friction and Lubricant in Metal Forming. *Lubricants*, 13(12), 512.